Spring 2017

Effects of PH20 Hyaluronidase Inhibition In Vivo Following Cerebral White Matter Injury

Rachel E. Siltman
Concordia University - Portland

Effects of PH20 Hyaluronidase Inhibition In Vivo Following Cerebral White Matter Injury

A senior thesis submitted to
The Department of Math-Science
College of Arts & Sciences

In partial fulfillment of the requirements
for a Bachelor of Arts degree in Biology

by

Rachel E. Siltman

Faculty Supervisor _____ _____
Dr. Rici Hallstrand **Date**

Department Chair _____ _____
Dr. Mihail Iordanov **Date**

Dean, College of Arts & Sciences _____ _____
Rev. Dr. David Kluth **Date**

Chief Academic Officer _____ _____
Dr. Joe Mannion **Date**

Concordia University
Portland, Oregon
May 2017

Table of Contents

To my father,
who first assured me "Scars are cool"

Acknowledgements

The completion of this thesis is thanks to all the people who have challenged, supported, and pushed me to pursue science and research. I am extremely fortunate to be part of a field that contributes substantially to human health.

To my faculty supervisor, Dr. Rici Hallstrand, my gratitude is immense. She continually supported and facilitated my efforts and growth in academia. I am thankful for her encouragement to participate in collaborative research and to share my findings at conferences. I owe thanks to committee members, Dr. Bert Coltman and Dr. Wayne Tschetter, whose contribution to this paper does not go unrecognized. As for my inspiration for tackling a thesis, I owe that to Dr. Charles Kunert for encouraging me to challenge myself and seek answers. More generally, to the professors Concordia has been fortunate to have, thank you for making contributions to my individual and academic growth.

I owe thanks to the M. J. Murdock Charitable Trust for funding and supporting my time at Oregon Health and Science University. To Dr. Stephen Back, I am privileged to know such a hardworking, life-long learner. Your guidance and wisdom will never be forgotten. To Dr. Taasin Srivastava, my appreciation is immeasurable as you have taught me the ways of the lab and how good science should be conducted and represented. For that, I am forever indebted. To the rest of the Back Lab, I am grateful for the mentorship and camaraderie. This work would not have been possible without their invaluable support and resources.

Finally, I must thank my family and friends for their love and encouragement. To my roommate, Kelly, your presence and friendship through this process will always be appreciated.

Abstract

Human infants born prematurely between 23-32 weeks have a predisposition toward sustaining white matter injury (WMI). In survivors of preterm birth, hypoxic-ischemic (H-I) damage to the cerebral white matter is the leading cause of a spectrum of neurological and motor deficits and in severe cases, cerebral palsy (CP). H-I triggers extracellular matrix (ECM) breakdown leading to production of inhibitory ECM components. H-I also induces vigorous proliferation of oligodendrocyte progenitor cells (OPCs) leading to accumulation of the pre-oligodendrocytes (preOLs). However, these preOLs fail to differentiate and generate myelin producing oligodendrocytes (OLs). Mechanistically, ECM breakdown blocks repair and regeneration of myelin following WMI as hyaluronic acid (HA), a major component of the brain ECM, is digested into bioactive fragments (fHA). Previous studies have shown that following WMI, HA degraded by PH20 hyaluronidase to fHA prevents differentiation of preOLs to mature OLs, but whether fHA plays a role in H-I mediated OPC proliferation is unknown. To determine if hyaluronidase plays a role *in vivo* to promote OPC proliferation, we utilized a neonatal rodent preterm model of H-I and a new selective PH20 inhibitor, SuBr3. Our hypothesis tests whether SuBr3 mediated inhibition of PH20 activity will also attenuate the OPC proliferation response observed after neonatal WMI. We found a significant decrease in $Ki67^{+}$ cells in WMI lesions in the SuBr3 treated animals relative to all other control groups, suggesting total cell proliferation was attenuated and mediated by PH20 hyaluronidase activity. Future experiments will analyze whether SuBr3 treatment also results in changes in the total pool of OL lineage cells and preOLs in the WMI lesions.

Introduction

Each year, an estimated 15 million babies are born premature (Blencowe et al., 2013). In the United States, ten percent of all live births per year are preterm (CDC, 2014). Despite new therapies, prematurity is the leading cause of abnormal brain maturation that is associated with impaired neurodevelopment in preterm neonates, including motor, cognitive, behavioral, or sensory deficits (Chau et al., 2013; Back and Miller, 2014; Back and Rosenberg, 2014). During human brain development, infants born between 23-32 weeks of gestation age have a predisposition toward white matter injury (WMI) (Back et al., 2001; Volpe, 2009). Preterm infants have a narrow auto-regulation window where cerebral blood flow (CBF) to the brain decreases when arterial blood pressure drops (Khwaja and Volpe, 2008). Inefficient or reduced oxygen and blood to the brain and lungs cause injury and is termed Hypoxia-Ischemia (H-I). Hence, WMI is triggered by an interaction of factors relating to cerebrovascular immaturity and impaired cerebral blood flow that cause complications during pre-term birth.

One of the hallmarks of WMI is myelination failure (Back and Rosenberg, 2014). Myelin is the insulation around the nerve fibers that allows quick transfer of information within the brain aiding in cognitive, motor and sensory functions. During human brain development, when neonates are most vulnerable to WMI (~23-32 gestation age), pre-myelinating oligodendrocytes (pre-OLs) are the dominant population in the brain (Back et al., 2001). Pre-OLs are the precursor glial cell to mature oligodendrocytes (OLs), a specialized glial cell that produces myelin. Pre-OLs are sensitive to H-I insults associated with WMI and pre-term birth (Back et al., 2001; Back et al., 2002; Craig et al., 2003; Back and Rosenberg, 2014). Thus, pre-term birth disrupts the inception of myelination as pre-

existing pre-OLs die and the newly born pre-OLs fail to mature to the next successive stage. Previous studies have defined the sequential maturation of the OL lineage into four distinct stages: oligodendrocyte progenitor cell (OPC), pre-OL, immature OL, and mature (myelinating) OL (Back et al., 2002) (***Fig. 1***).

The regeneration and repair story for myelin indicates that it is much more complex than research originally predicted. Previous studies have defined a novel mechanism of myelination failure that disrupts the sequential maturation of the OL lineage in WMI (Back et al., 2002). During the early phase of white matter brain injury, preOL death occurs. This phase is followed by a vigorous regenerative response of oligodendrocyte progenitor cells (OPCs) that re-expand the pre-oligodendrocyte (preOL) pool. However, these newly generated preOLs cease to differentiate, and the OL lineage fails to mature to the next successive stage (Segovia et al., 2008). Myelin is no longer generated. This abnormal proliferation and maturation of OLs contributes to aberrant brain repair after injury and has been linked to extracellular matrix (ECM) breakdown (Sherman et al., 2015).

ECM breakdown is considered one of the main events that influences myelination failure following WMI, but the molecular mechanisms are poorly defined (Lau et al., 2013). The brain ECM regulates the central nervous system (CNS) in diverse ways and significant changes in its physiology have consequences to its function. WMI compromises the integrity of the blood-brain barrier (BBB) and the endothelial cells lining the blood vessels break down leading to monocyte infiltration and reactive gliosis (Shechter et al., 2013). A glial scar forms in response to reactive astrogliosis from the demyelinating white matter. Reactive astrogliosis is characterized by proliferating astrocytes as a maladaptive response to altered ECM homeostasis. Furthermore, this newly formed glial scar produces

an abnormal ECM as it contains altered levels of hyaluronic acid (HA) (Back et al., 2005). Hence, WMI induced ECM remodeling generates an altered micro-environment that ultimately attenuates remyelination and repair.

Hyaluronic acid (HA) is a prominent component of the brain ECM that provides structural and functional support thereby regulating cellular homeostasis (Rauch, 2004). HA is a glycosaminoglycan composed of disaccharide units of glucuronic acid and N-acetyl-D-glucosamine synthesized by transmembrane synthases (Sherman and Back, 2008). WMI results in the formation of the glial scar containing altered levels of HA, indicating that HA can play a significant role in influencing myelin repair. Furthermore, experiments have shown that remyelination failure is due to accumulation of a specific high molecular weight (HMW) form of HA synthesized by reactive proliferating astrocytes (astrogliosis) and other microglial cells within the lesions (Back et al., 2005).

HMW forms of HA found in the white matter lesions have been proposed to be digested into bioactive forms by a selective hyaluronidase enzyme, PH20, found in the CNS (Preston et al., 2013). This generation of digested bioactive HA fragments (fHA) by PH20 hyaluronidase is responsible for arresting preOL maturation following injury in an adult rodent model of demyelination. Correspondingly, an elevated expression of PH20 hyaluronidase was found in the demyelinated brain lesions. Understanding the molecular mechanisms mediated by PH20 will aid in development of possible therapies to promote regeneration and repair following neonatal WMI. Degradation of HMW-HA by hyaluronidases stimulates cell proliferation (Su et al., 2017) and similarly, WMI induces proliferation of glial cells as well as OPCs (Segovia et al., 2008); it is not clear whether WMI induced HMW-HA breakdown can also influence OPC proliferation.

Using a neonatal rodent pre-term equivalent model of Hypoxia-Ischemia, we tested whether blocking HMW-HA degradation can influence myelination and repair following WMI. This rodent model successfully emulates all the defining features of WMI observed in human patients namely, ECM breakdown, OPC proliferation and OL maturation arrest. Similar to human preterm WMI, the lesions generated by our well-established neonatal rodent H-I model are also highly enriched in $GFAP^+$ reactive astrocytes and display marked elevations in staining for HA that coincide with extensive myelination failure. Previous studies have been able to promote oligodendrocyte maturation using general hyaluronidase inhibitors *in vitro* (Preston et al., 2013). We investigated the molecular mechanisms influencing OPC proliferation following WMI by employing an *in vivo* approach using a new selective hyaluronidase inhibitor, SuBr3, that prevents HMW-HA breakdown. Our preliminary studies reveal that SuBr3 treatment attenuates the proliferation of cells in H-I induced white matter lesions thereby implicating influence of HMW-HA breakdown on cell cycle. Hence, the use of this new selective hyaluronidase inhibitor, SuBr3, will allow us to provide further insights into strategies to promote preOL maturation that ultimately improve the neurological outcome for children with neurodevelopmental disabilities related to preterm birth.

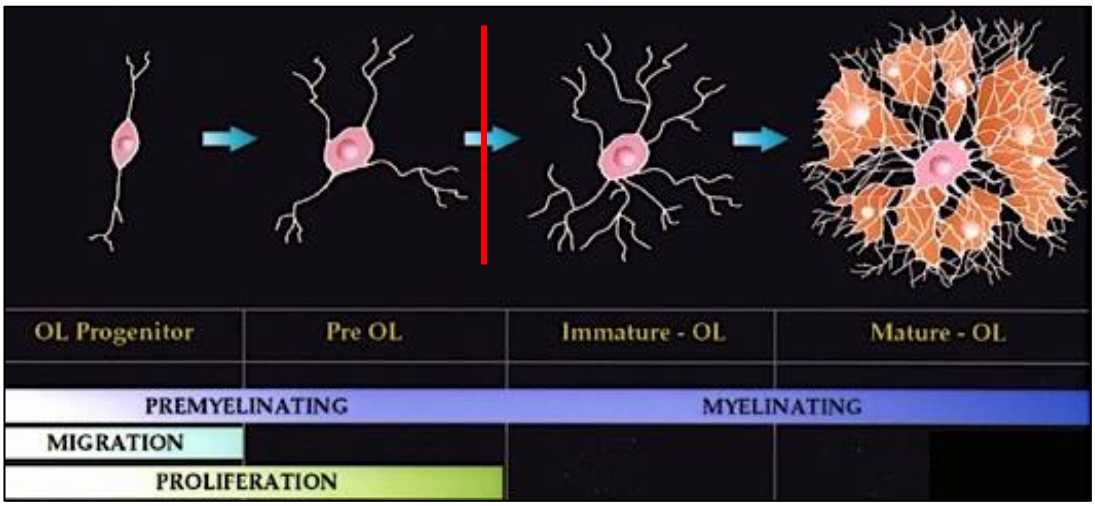

Figure 1. The four sequential stages of the oligodendrocyte (OL) lineage after white matter injury (WMI). The red line indicates failure of pre-oligodendrocytes (preOLs) to differentiate and generate myelin after a vigorous proliferation of oligodendrocyte progenitor cells (OPCs) that expand the preOL pool (Back et. al 2002).

Materials and Methods:

Animal Surgical Procedures

All animal measures were approved by the OHSU Institutional Animal Care and Use Committee (IACUC) according to the NIH Guide for the Care and Use of Laboratory Animals. Timed pregnant Sprague-Dawley (SD) rats were purchased from Charles River (Hollister, CA, USA). At postnatal day 3 (P3), animals were anaesthetized and received a single injection of 2μM SuBr3 (final concentration) or equivalent volume of vehicle (DMSO) into the left hemisphere. This was immediately followed a hypoxic-ischemic protocol with the left common carotid artery ligation (10 pups/litter) to generate focal cerebral injury lateralized to one hemisphere with the contralateral hemisphere serving as a control (Vannucci, 1999; Segovia et. al, 2008). Following a minimum of 1h recovery with their dams, pups were placed into containers (submerged into a 37^{o}C water bath to maintain normothermia) aerated with humidified oxygen (6% for 3.5h) and balanced nitrogen at 3 L/min. The pups were then returned to their dams until sacrifice (Hypoxia-Ischemia [H-I] group). Animals survived for 4 days (until P7). A set of animals were also recovered without receiving surgery/ischemia and were treated as un-injured controls.

Animals were sacrificed by decapitation following anesthesia. The brains were quickly dissected out and assessed for the presence of lesions. Only brains exhibiting well-defined brain lesions were included in this study. A set of lesioned brains were collected and fixed in 4% paraformaldehyde (PFA; 0.1 M phosphate buffered saline [PBS]) for 2 days at 4^{o}C, followed by thorough PBS washing for immunohistochemistry (IHC). For each experimental outcome, a minimum of three brain sections were used for each group (**Fig. 2**).

Immunohistochemistry

Single- or double-labeling immunofluorescence was performed on 50μM thick brain sections cut with a Vibratome (Leica VT1000) in 24-well plates. Antibodies and dilutions were as follows: mouse polyclonal anti-GFAP (1:500; EMD Millipore), rabbit polyclonal anti-Ki67 (1:100; Leica, USA), and mouse monoclonal anti-olig2 (1:250; Dr. John Alberta, Dana-Farber Cancer Institute, Boston, MA, USA). For all the antibodies used the sections underwent the antigen retrieval procedure wherein the sections were incubated in 0.01 M citrate buffer (pH 6.0) at 85°C for 15 min, left to cool for 10 min, and then washed three times in PBS. For labeling, sections were blocked for 1h in PBS containing 5% normal goat serum (NGS), and then with primary antibodies diluted in PBS/3% NGS for 3-4 nights at 4°C. Blocking and primary antibody incubation was performed with 0.4% triton X-100 (Sigma-Aldrich Co.). For secondary detection, all sections were washed three times in PBS, and incubated with appropriate fluorescent dye conjugated secondary antibodies (Jackson Research Labs). Nuclei were counterstained with DAPI (Invitrogen Co.). Sections were mounted with Vectashield fluorescent mounting medium (Vector Laboratories, Inc., Burlingame, CA, USA).

Quantification of Total Cell Count of GFAP$^+$ and Ki67$^+$-labeled Cells

The white matter of sectioned tissue slices was analyzed using a Ziess Imager.M2 microscope (Carl Ziess Microscopy, Thornwood, NY, USA) coupled to a Stereo-Investigator (SI) stereology system (MBF Bioscience, Williston, VT, USA). For each histological (serial) section slice, the superior corpus callosum (defined by DAPI-staining) region of interest (ROI) was traced at 5x magnification. Using the software to maintain

white matter boundaries, GFAP$^+$ and Ki67$^+$-labeled cells were estimated in the superior corpus callosum using the Optical Fractionator probe (Counting frame, 40×40μm; z-depth, 20μm) at 100X oil magnification. Cells were counted in a minimum of three adjacent coronal sections (300μm apart) in lesions and their corresponding control regions in the contralateral hemisphere. A minimum of 20 randomly selected white matter fields was counted per slice. The slice thickness was also measured at each counting site. The total number of counted nucleus profiles comprised the calculation of the total cell count.

Quantification of Total Cell Count of Olig2$^+$, Ki67$^+$, Olig2$^+$-Ki67$^+$-labeled Cells

From the same perinatal rodents, tissue sections were immunofluorescently double-labeled for Olig2 and Ki67. Quantification of total Olig2$^+$, Ki67$^+$ and Olig2$^+$-Ki67$^+$-labeled cells was determined in tissue sections with the same regional boundaries as GFAP$^+$ or Ki67$^+$-labeled cells. Lesion hemispheres were identified via histology by typical reactive appearance of early OL progenitors plus preOL and OL death. The white matter of sectioned tissue slices was analyzed using the same Ziess Imager.M2 microscope coupled to a SI stereology system. Cell profiles were counted with a 100X objective. For each slice, the superior corpus callosum was traced at 5x magnification. Using SI stereology system to maintain white matter boundaries, three separate markers were used to make cells counts for Olig2$^+$, Ki67$^+$ and double-labeled Olig2$^+$-Ki67$^+$ cells. Cells were estimated in the superior corpus callosum using the Optical Fractionator probe (Counting frame, 40×40μm; z-depth, 20μm) at 100X oil magnification. Because of the complexity of injury in animals, each coronal section was categorized A, B, or C signifying the location of sections in the brain as rostral, medial, or caudal respectively. A minimum of 20 randomly selected white matter fields was counted per slice and slice thickness was measured at each counting site.

The total number of counted nucleus profiles of OL lineage cells comprised the calculation of the total cell count.

Image and Statistical Analysis

Microscope images were analyzed using Fiji ImageJ software. Data from slice counts were analyzed using multiple comparisons with ordinary one-way ANOVA with Prism Version 7.0 (GraphPad Software, Inc., La Jolla, CA, USA). All data were normally distributed and expressed as standard error of mean (+/- SEM). To determine the effect of H-I on total cell measurements, we used mean cerebral thickness as a marker for spatial distribution of total cell count. For each lesion and corresponding contralateral control region, cerebral thickness was measured between first and last nucleus in focus within counting grid of the SI stereology probe. Three thickness measurements were obtained at the medial, midpoint, and lateral boundaries of the lesion within the superior corpus callosum contoured region of interest (ROI). First, data analysis was performed on each individual animal case within H-I groups (DMSO H-I and SuBr3 H-I) between H-I lesion and the contralateral control hemisphere. Because biological variability exists between animals, we accounted for the degree of injury between each individual animal when comparing total cells counts between treatment groups. Multiple comparisons with ordinary one-way ANOVA was run between pooled control and H-I groups to determine relative cell loss due to induced H-I. Means with error bars are presented in all figures with significance indicated for statistical analyses. A p-value less than 0.05 was considered statistically significant. (For all figures, $*p < 0.05$, $**p < 0.01$, $***p < 0.001$ refer to analysis of data significance for cerebral cell loss between groups.)

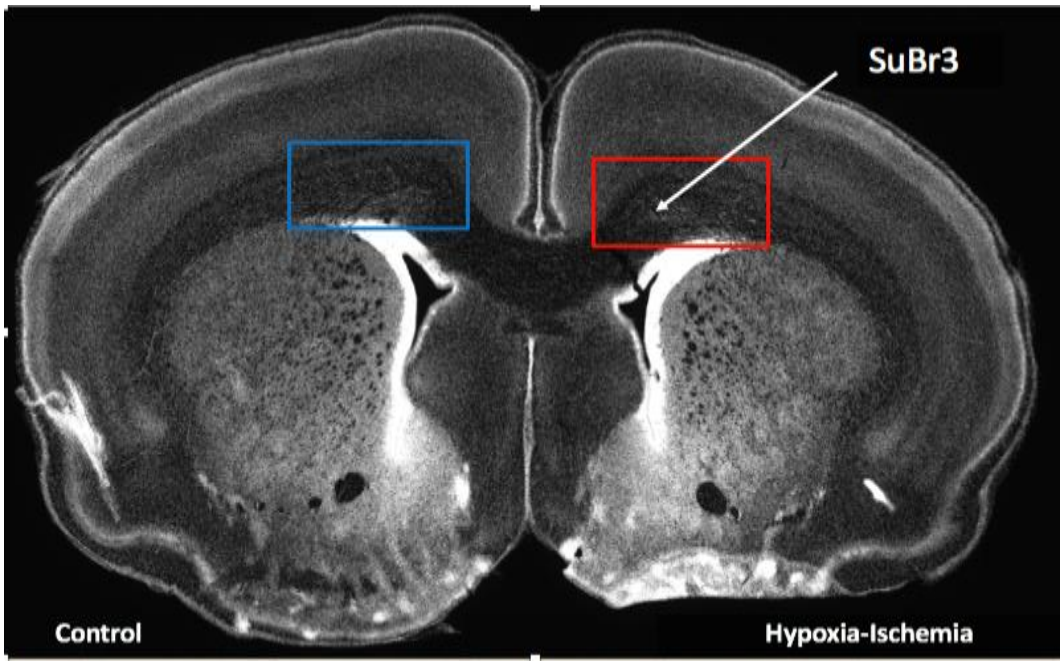

Figure 2. Hypoxic-ischemic (H-I) brain tissue cut on coronal plane with a Vibratome (Leica VT1000). Representative image of the area of counting in the superior corpus callosum (CC) of SuBr3-injected (2μM) animals. The blue and red box indicates area of counting in the control and lesion hemisphere, respectively. The white arrow indicates injection site of SuBr3 in lesion hemisphere.

Results

Using Reactive Astrogliosis to define WMI induced lesions following Hypoxia-Ischemia

Previous studies using post-mortem tissue derived from preterm human infants suggest that arrested maturation of preOLs is associated with ECM remodeling leading to HA accumulation and reactive gliosis (Buser et al., 2012). Our preterm equivalent rodent model also undergoes preOL arrest following H-I (Segovia et al., 2008) but whether this is accompanied with ECM remodeling leading to changes in HA levels in the neonatal lesions remains unknown. To study mechanisms of ECM remodeling in the lesions we first defined the H-I induced lesions. We used GFAP as a marker for defining the H-I induced lesion as elevated astrocyte expression in response to H-I corresponds to injury *in vivo* (Lyck et al., 2008). We determined the severity of injury in animals given either SuBr3 (to block ECM remodeling) or Vehicle (DMSO) and then subjected to H-I. In the SuBr3 group, the population of $GFAP^+$-labeled astrocytes increased in lesioned areas compared to corresponding contralateral control region (**Fig. 3**). And the same was the case with DMSO H-I group (B1-B3) (**Fig. 4**). Increase in $GFAP^+$ astrocytes in both the groups (DMSO and SuBr3) following H-I indicates that the lesions were induced following injury.

We also observed biological variability within the SuBr3 and DMSO H-I experimental groups. Cell counts from Animal A2* do not reflect injury after H-I (**Fig. 3**). In fact, we observed a downward trend in the total cell count of the lesioned hemisphere compared to the contralateral control hemisphere, which could be increased cell death or cell migration following H-I. After review, we found the lesion as defined by $GFAP^+$ astrocytes fell outside the region of counting defined within the superior corpus callosum (**Fig. 2**). Because we used a conservative systematic sampling approach via stereology,

lesions outside the counting region will not reflect injury, however, we did confirm injury through histology. Similarly, in the DMSO H-I group animal B3, the contralateral un-lesioned hemisphere had variable expression of $GFAP^+$ astrocytes (Fig.4). Hence, these results helped us narrow down the cohort of animals that had sustained WMI following H-I that we then utilized for our subsequent analysis for ECM remodeling and its effects on preOL maturation.

SuBr3 Attenuates Total Cell Proliferation after Hypoxia-Ischemia

ECM remodeling induced breakdown of HA by hyaluronidases leads to cell proliferation (Su et al., 2017). In our preterm equivalent rodent model, H-I apart from inducing preOL arrest also induces OPC proliferation (Segovia et al., 2008). It remains unknown whether ECM remodeling is linked to regulating OPC proliferation in our rodent model following H-I. Using a new class of selective hyaluronidase inhibitor, SuBr3, we investigated if HA breakdown regulates cell proliferation. After confirming the lesions in the different experimental and control groups with GFAP, proliferating cells within these lesions were identified with the cycle-cell proliferation marker Ki67 (Scholzen and Gerdes, 2000). The lesions in the DMSO H-I group displayed a non-significant increase in the total number of $Ki67^+$ cells **(Fig.6)** suggesting that injury promotes cell proliferation. Importantly, these results indicate that DMSO treatment itself does not influence cell proliferation following injury. In contrast, total population of $Ki67^+$ cells decreased in lesioned hemisphere compared to corresponding contralateral control hemisphere in individual SuBr3 H-I animals except for A3* (**Fig. 5**).

Since the animals were stereotactically injected with either DMSO or SuBr3 prior to being subjected to H-I and the injection procedure itself can induce injury mediated cell proliferation, we next compared the total numbers of $Ki67^+$ cells amongst all the control and experimental groups: True Controls (animals that did not undergo H-I or ICV injections; n=2), DMSO Control (animals that received DMSO ICV injections only; n=2), DMSO H-I (animals that received DMSO ICV injections and also underwent H-I; n=3), and SuBr3 Control (animal that received SuBr3 ICV injection only; n=2) and SuBr3 H-I (animals that received SuBr3 ICV injections and also underwent H-I; n=4) (**Fig. 8**). Compared to DMSO H-I group, total $Ki67^+$ cell counts in the SuBr3 H-I group were significantly decreased (**Fig. 8**). Collectively, these results support that SuBr3 selectively blocks a cell proliferative response in the white matter lesions generated by H-I and this may be linked to HA breakdown.

Does SuBr3 Influence OPC Proliferation Following H-I?

H-I at P3 leads to reactive gliosis and OPC proliferation (Segovia et al., 2008) whereas SuBr3 treatment prior to H-I appears to attenuate total cell proliferation (**Fig. 7**); we next examined whether SuBr3 attenuated H-I induced OPC proliferation. To this end, the lesions from animals with confirmed WMI (**Fig. 3** and **Fig. 4**) were double stained with Olig2 (labels the OL lineage cells) and Ki67 to determine proliferating OPCs.

We compared the total number of $Olig2^+$ and $Olig2^+$-$Ki67^+$-labeled cells in our control and experimental groups (**Fig.8**). Analyzing only $Olig2^+$ cells, we determined that cell counts were significantly decreased in the SuBr3 H-I cell compared to the DMSO H-I group (**Fig. 9A**). This suggested that the SuBr3 influenced either the survival or

proliferation of OL lineage cells. We next examined the total numbers of proliferating OPCs by counting $Olig2^{+}$-$Ki67^{+}$ double labeled cells, but we were not able to detect any significant differences between the control and experimental groups (**Fig. 9B**). Collectively, these results suggest that attenuating HA breakdown following WMI by SuBr3 treatment may influence survival of OL lineage cells suggesting that under conditions of injury hyaluronidase activity may also play a protective role. It is not clear from our data regarding the identity of the glial or neuronal cell type whose proliferation is regulated by hyaluronidase activity as SuBr3 treatment attenuates the total pool of proliferating cells. Future studies, using a bigger cohort of animals and SuBr3 will examine all the cell types whose proliferation could be influenced by WMI.

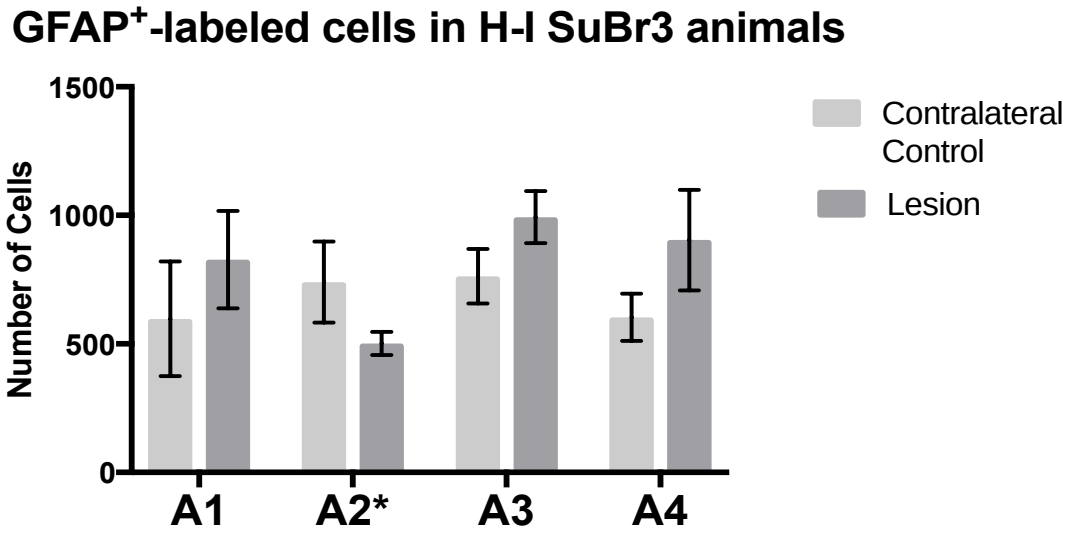

Figure 3. Total GFAP-labeled cells in superior corpus callosum of four H-I injected SuBr3 animals. Total population of $GFAP^{+}$-labeled astrocytes increased in lesioned areas compared to corresponding contralateral control region, however, treated animals displayed no significant difference in total cell counts between the lesion and corresponding contralateral control hemisphere (n=4). Confirmed injury through histology.

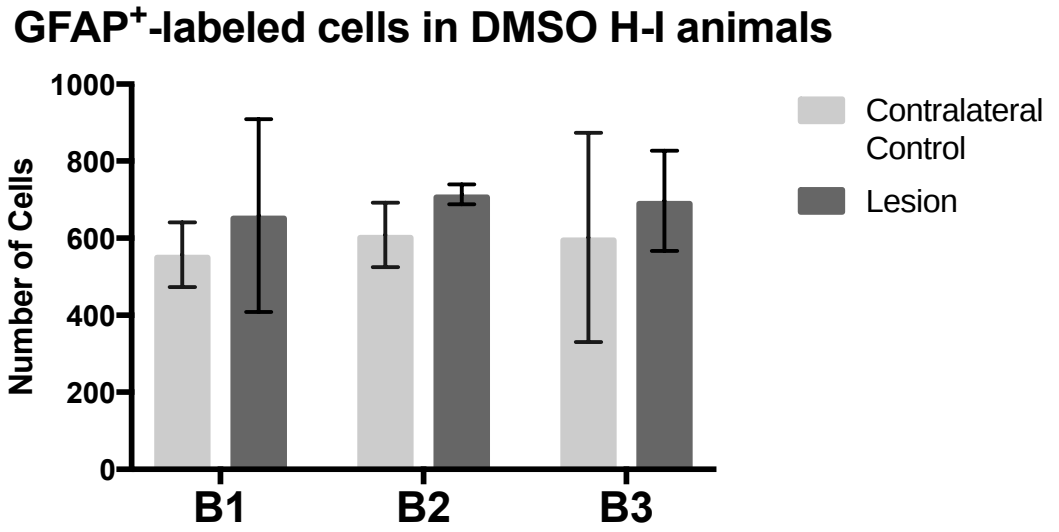

Figure 4. Total GFAP-labeled cells in superior corpus callosum of H-I injected DMSO animals. Total population of $GFAP^{+}$-labeled astrocytes increased in lesioned areas compared to corresponding contralateral control region (n=3).

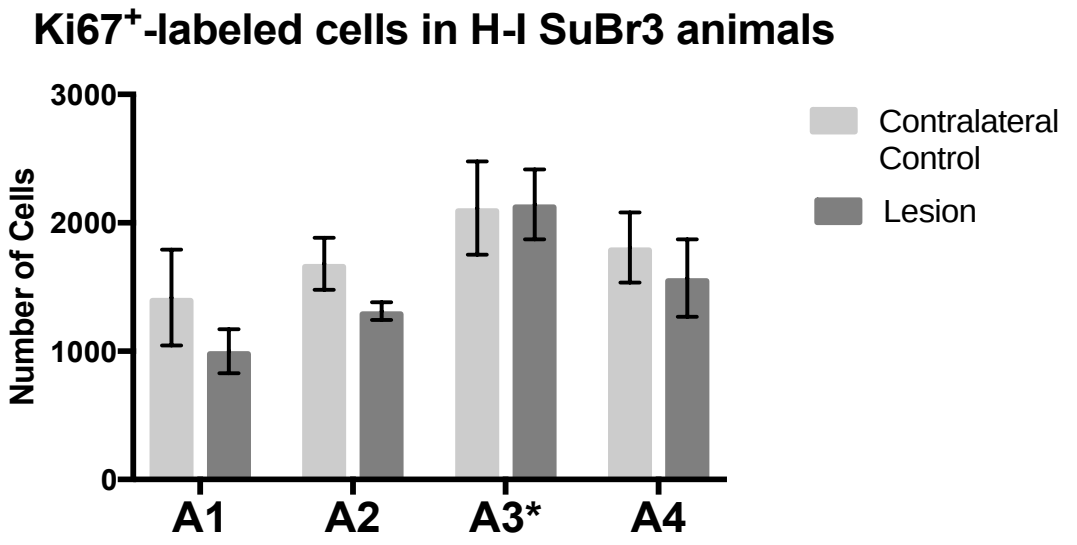

Figure 5. Total Ki-67 labeled cells in superior corpus callosum in same four H-I SuBr3 animals. Total population of $Ki67^{+}$-labeled cells decreased in lesioned hemisphere compared to corresponding contralateral control hemisphere in H-I injected SuBr3 animals (n=4).

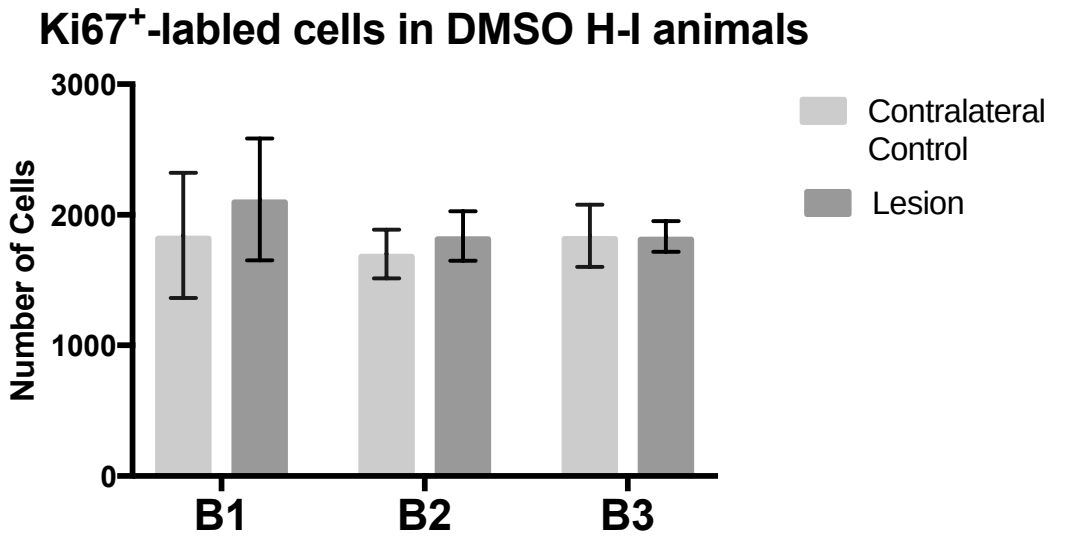

Figure 6. Total Ki-67 labeled cells in superior corpus callosum in same H-I DMSO animals. Total population of $Ki67^{+}$-labeled cells was similar between lesioned hemisphere and corresponding contralateral control hemisphere. DMSO alone did not have an effect on total cell proliferation. Total cell counts were non-significant (n=3).

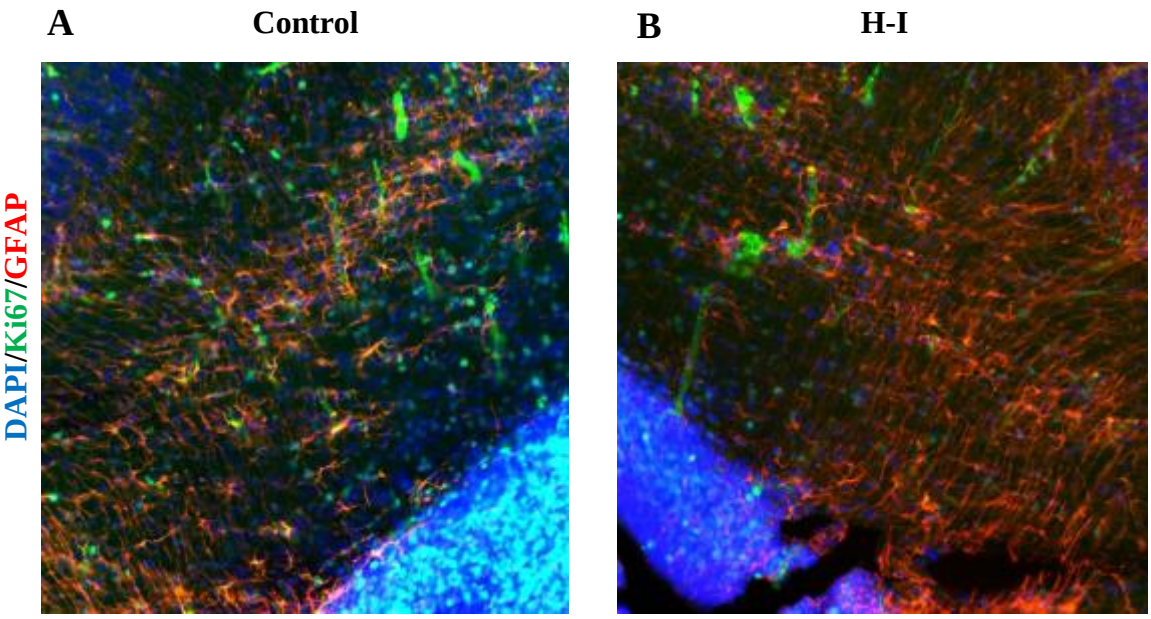

Figure 7. Representative images of the corpus callosum (CC) from rats that sustained WMI. Brain tissues were fixed and stained with glial fibrillary acidic protein (GFAP; red; to label astrocytes), cell-cycle marker (Ki67; green; to label cell proliferation), and 4′, 6- diamidino-2-phenyl-inodole (DAPI; blue; to label nuclei). To block hyaluronidase activity, animals were treated with SuBr3 (2μM). A) There is an increased localization of $Ki67^{+}$ cells but decreased $GFAP^{+}$ astrocytes in Control hemisphere and B) a decreased localization of $Ki67^{+}$ cells and increased $GFAP^{+}$ astrocytes in H-I hemisphere.

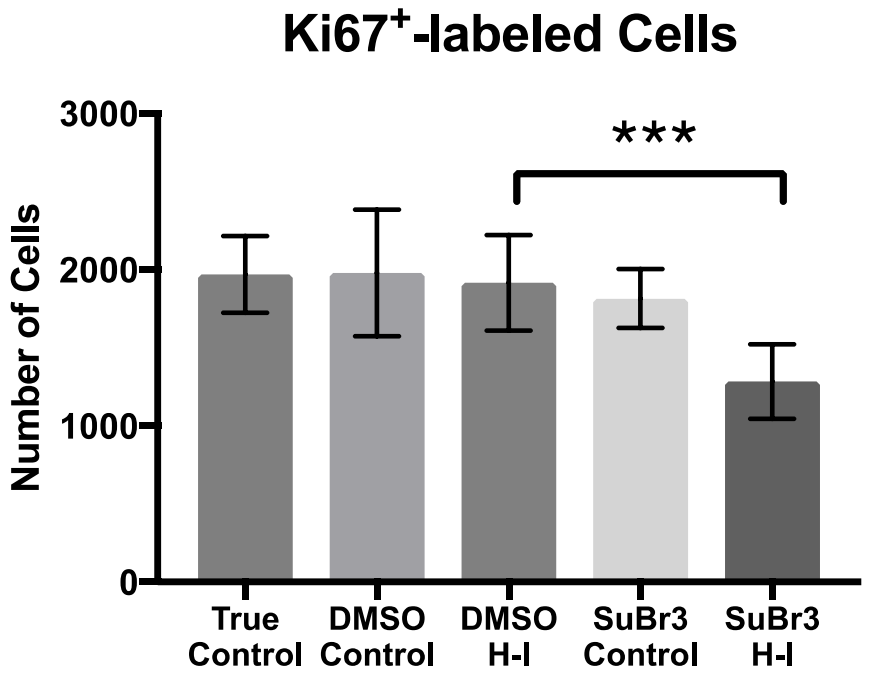

Figure 8. Combined mean Ki-67^{+}-labeled cells in lesion hemisphere of H-I SuBr3 animals compared to all other control groups: True Control (n=2 animals), DMSO Control (n=2 animals), DMSO H-I (n=3 animals), and SuBr3 Control (n=1 animals). Total cell counts in SuBr3 injected H-I lesion animals significantly decreased relative to DMSO H-I (***p=0.0007).

A.

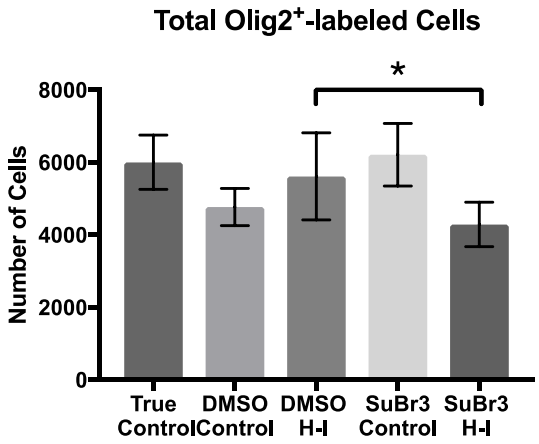

B.

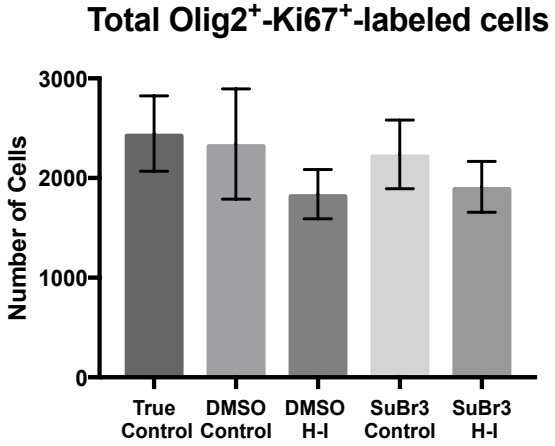

Figure 9. A) Pooled mean Olig2^{+}-labeled counts in control groups: True Control (n=2 animals), DMSO Control (n=1 animals), DMSO H-I (n=3 animals), and SuBr3 Control (n=1 animals) compared to SuBr3 H-I animals (n=3 animals). SuBr3 H-I cell counts decreased significantly compared to DMSO H-I (*p=0.0123). B) Pooled Olig2^{+}-Ki67^{+}-labeled cell counts were non-significant between the control and experimental groups.

Discussion

Previous report from our lab has linked accumulation of HA and myelination failure that disrupts the maturation of the OL cell lineage in pre-term human neonates (Buser et al., 2012) (**Fig. 1**). WMI triggers neuronal and glial cell death, but the developing brain induces both migration and proliferation of OPCs into the white matter lesions resulting in expansion of the preOL pool. However, these newly formed preOLs then fail to mature into myelin producing OLs. Thus, myelination failure and breakdown of the ECM contributes to abnormal brain repair after WMI (Back and Rosenberg, 2014). By employing a new selective hyaluronidase inhibitor, SuBr3, we investigated the potential outcomes of attenuating ECM breakdown following WMI *in vivo*. Our present study suggests that HMW-HA breakdown *in vivo* regulates cell proliferation in the white matter lesions.

Although ECM breakdown is one of the main events that coordinates the events leading to myelination failure following WMI, the molecular mechanisms remain poorly defined (Lau et al., 2013). HMW-HA in its intact form negatively regulates cell proliferation by its breakdown either via hyaluronidase activity or oxidative stress promotes cell proliferation (Morrison et al., 2001; Preston and Sherman, 2013; Su et al., 2016). A previous study utilizing an adult rodent model of WMI implicated PH20 hyaluronidase in preventing the differentiation of preOLs to mature OLs (Preston et. al, 2013). That study relied on a general hyaluronidase inhibitor, which could potentially have off target effects and it also did not address whether ECM modification plays a role in OPC proliferation following WMI. To investigate the molecular mechanisms influencing OPC proliferation following WMI we took advantage of our rodent pre-term equivalent model

and tested a more selective hyaluronidase inhibitor, SuBr3. This inhibitor (SuBr3) is derived from apigenin (compounds with well-known anti-hyaluronidase activity) and has a flavonoid modification for increased solubility and efficacy (Srinavasa et al., 2014). We observed reduced number of proliferating cells in response to SuBr3 treatment *in vivo.* Specifically, the SuBr3 treated animals displayed a decrease in $Ki67^+$ proliferating cells in lesioned hemispheres compared to corresponding contralateral control hemispheres (**Fig. 5**). Furthermore, combined mean cell counts for $Ki67^+$ cells in SuBr3 H-I lesion hemispheres decreased significantly compared to all other control groups (**Fig. 8**). Collectively, these results support that SuBr3 selectively blocks a cell proliferative response in the white matter lesions generated by H-I. Hence, these results suggest a mechanistic link between HMW-HA breakdown and OPC proliferation *in vivo*.

Since WMI drives cell proliferation of OPCs *in vivo* (Segovia et al., 2008), we determined whether SuBr3 treatment could influence this event. We determined the total numbers of proliferating OPCs by counting $Olig2^+$-$Ki67^+$ double labeled cells, but were not able to detect any significant differences between the control and experimental groups (**Fig. 9B**). Surprisingly, we observed a significant decrease in the $Olig2^+$-labeled cell population in SuBr3 treated animals compared to DMSO treated animals (**Fig. 9A**). Although the cohort of animals utilized for this preliminary study is small, nevertheless, these observations suggest that HMW-HA breakdown following WMI apart from regulating cell proliferation could also either influence the survival or migration of OL lineage cells in the WM lesions.

Overall our findings indicate that the PH20 inhibitor, SuBr3, can be utilized to provide new insights into mechanisms that block normal myelination, and, thereby could

be helpful in developing new therapies to reverse arrested white matter maturation in survivors of premature birth. Since remyelination requires repair of the ECM and the sequential maturation of OL lineage in the WM lesions, it is critical to investigate the mechanisms following WMI by employing *in vivo* approaches. Since Olig2 labels all the cells of the OL lineage irrespective of their developmental stage, future experiments will analyze SuBr3 treatment utilizing a larger cohort of animals and OL cell stage specific markers in H-I lesions. Potential roles for hyaluronidase activity either in OL cell survival or migration will also be explored by using selective markers for cell death and migration. Additionally, future studies will attempt to define a time point in which analysis of both proliferating and arrested preOLs can be performed when the drug is administered. These efforts will provide further insights into strategies to promote preOL maturation that ultimately improve the neurological outcome for children with neurodevelopmental disabilities related to preterm birth.

References

Back, S. A., Luo, N. L., Borenstein, N. S., Levine, J. M., Volpe, J. J., & Kinney, H. C. (2001). Late oligodendrocyte progenitors coincide with the developmental window of vulnerability for human perinatal white matter injury. *J Neurosci*. 21(4), 1302–1312.

Back, S. A., Han, B. H., Luo, N. L., Chricton, C. A., Xanthoudakis, S., Tam, J., Arvin, K. L., & Holtzman, D. M. (2002). Selective vulnerability of late oligodendrocyte progenitors to hypoxia–ischemia. *J Neurosci*, 22(2), 455-463.

Back, S. A., Tuohy, T. M., Chen, H., Wallingford, N., Craig, A., Struve, J., … Sherman, L. S. (2005). Hyaluronan accumulates in demyelinated lesions and inhibits oligodendrocyte progenitor maturation. *Nature Medicine,* 11(9), 966 – 972.

Back, S. A. & Miller, S. P. (2014). Brain injury in premature neonates: A primary cerebral dysmaturation disorder? *Annals of Neurology*, 75(4), 469–486.

Back, S. A. & Rosenberg, P.A. (2014). Pathophysiology of glia in perinatal white matter injury. Glia; 62(11), 1790-1815.

Blencowe, H., Cousens, S., Chou, D., Oestergaard, M., Say, L., Moller, A.-B., … Lawn, J. (2013). Born Too Soon: The global epidemiology of 15 million preterm births. *Reproductive Health*, *10*(Suppl 1), S2.

Buser, J. R., Maire, J., Riddle, A., Gong, X., Nguyen, T., Nelson, K., …Stephen, S. A. (2012). Arrested preoligodendrocyte maturation contributes to myelination failure in premature infants. *Ann Neurol*, 71(2), 93–109.

Centers for Disease Control and Prevention. (2010). Preterm birth. Retrieved from http://www.cdc.gov/reproductivehealth/maternalinfanthealth/pretermbirth.htm

Chau, V., Synnes, A., Grunau, R. E., Poskitt, K. J., Brant, R., & Miller, S. P. (2013). Abnormal brain maturation in preterm neonates associated with adverse developmental outcomes. *Neurology*, *81*(24), 2082–2089.

Craig, A., Luo, N. L., Beardsley, D. J., Wingate-Pearse, N., Walker, D. W., Hohimer, A. R., & Back, S. A. (2003). Quantitative analysis of perinatal rodent oligodendrocyte lineage progression and its correlation with human. *Exp. Neurol*, 181(2), 231–240.

Dean, J. M., Riddle, A., Maire, J., Hansen, K. D., Preston, M., Barnes, A. P., … Back, S. A. (2011). An organotypic slice culture model of chronic white matter injury with maturation arrest of oligodendrocyte progenitors. *Molecular Neurodegeneration*, *6(1)*, [46].

Khwaja, O., & Volpe, J. J. (2008). Pathogenesis of cerebral white matter injury of prematurity. *Archives of Disease in Childhood. Fetal and Neonatal Edition*, *93*(2), F153–F161.

Lau, L. W., Cua, R., Keough, M. B., Haylock-Jacobs, S., & Yong, V. W. (2013). Pathophysiology of the brain extracellular matrix: a new target for remyelination. *Nature Reviews Neuroscience*, 14(10), 722–729.

Lyck, L., Dalmau, I., Chemnitz, J., Finsen, B., & Schrøder, H. D. (2008). Immunohistochemical markers for quantitative studies of neurons and glia in human neocortex. *J Histo Cytochem*, *56*(3), 201–221.

Morrison, H., Sherman, L.S., Legg, J., Banine, F., Isacke, C., Haipek, C.A.,…Herrlich, P. (2001). The NF2 tumor suppressor gene product, merlin, mediates contact inhibition of growth through interactions with CD44. *Genes Dev*, 15(8), 968–980.

Preston, M., Gong, X., Su, W., Matsumoto, S. G., Banine, F., Winkler, C., … Sherman, L. S. (2013). Digestion products of the ph20 hyaluronidase inhibit remyelination. *Annals of Neurology*, *73*(2), 266–280.

Rauch, U. (2004). Extracellular matrix components associated with remodeling processes in brain. *Cellular and Molecular Life Sciences*, 61(16), 2031–2045.

Scholzen, T. & Gerdes, J. (2000). The Ki-67 protein: from the known and the unknown. *J Cell Physiol*, 182(3), 311–322.

Segovia, K. N., McClure, M., Moravec, M., Luo, N. L., Wan, Y., Gong, X., … Back, S. A. (2008). Arrested oligodendrocyte lineage maturation in chronic perinatal white matter injury. *Annals of Neurology*, *63*(4), 520–530.

Shechter, R., Miller, O., Yovel, G., Rosenzweig, N., London, A., Ruckh, J., … Schwartz, M. (2013). Recruitment of beneficial M2 macrophages to injured spinal cord is orchestrated by remote brain choroid plexus. *Immunity*, *38*(3), 555–569.

Sherman, L. S., and Back, S.A. (2008). A 'GAG' reflex prevents repair of the damaged CNS. *Trends Neurosci*. 31(1), 44–52.

Sherman, L., Matsumoto, S., Su, W., Srivastava, T., & Back, S. A. (2015). Hyaluronan synthesis, catabolism, and signaling in neurodegenerative diseases. *International Journal of Cell Biology*, vol. 2015, Article ID 368584, 1-10.

Srinivasa, V., Sundaram, M. S., Anusha, S., Hemshekhar, M., Chandra Nayaka, S., Kemparaju, K.,…Rangappa, K. S. (2014). Novel Apigenin Based Small Molecule that Targets Snake Venom Metalloproteases. *PLoS ONE* 9(9): e106364.

Su, W., Foster, S., Xing, R., Feistel, K., Olsen, R., Acevedo, S., … Sherman, L. (2017). CD44 transmembrane receptor and hyaluronan regulate adult hippocampal neural stem cell quiescence and differentiation. *J Biol Chem*, 292(11), 4434-4445.

Vannucci, R. C., Connor, J. R., Mauger, D. T., Palmer, C., Smith, M. B., Towfighi, J., & Vannucci, S. J. (1999). Rat model of perinatal hypoxic-ischemic brain damage. *J Neurosci Res*, 55(2), 158 –163.

Volpe, J. J. (2001). Neurobiology of periventricular leukomalacia in the premature infant. *Pediatr Res*, 50, 553–56.

Volpe, J. J. (2009). Brain injury in premature infants: a complex amalgam of destructive and developmental disturbances. *Lancet Neurol*, 8, 110–124.